

Quasi-Mössbauer effect in two dimensions

Dennis D. Dietrich and Lester L. Hirst*

*Institut für Theoretische Physik, Johann Wolfgang Goethe-Universität,
60054 Frankfurt am Main, Germany*

Abstract

Expressions for the absorption spectrum of a nucleus in a three- and a two-dimensional crystal respectively are obtained analytically at zero and at finite temperature respectively. It is found that for finite temperature in two dimensions the Mössbauer effect vanishes but is replaced by what we call a Quasi-Mössbauer effect. Possibilities to identify two-dimensional elastic behavior are discussed.

arXiv:cond-mat/0401423v2 [cond-mat.other] 11 Feb 2004

* deceased

I. INTRODUCTION

In nuclear reactions, the atoms usually are treated as free, i.e., unbound. The chemical bonds between each other are neglected. This is justified with the argument that the typical energy in a nuclear process is generally much higher than the chemical binding energies (1 to 10 eV) and moreso than that of lattice vibrations (10^{-2} to 10^{-1} eV)¹. In return, most of the detailed qualities of the nucleus are of secondary importance in solid state physics.

These assumptions are not correct without limitations. Consider for example the absorption or emission of γ -photons by nuclei. During absorption processes (emission analogously) the nucleus first is in a ground state and makes a transition into an excited state. The energy difference between the ground and the excited state is not constant. It has a certain distribution which is linked to the life-time of the excited state by Heisenberg's uncertainty relation. For these reactions the difference has values between 10^{-11} to 10^{-6} eV¹. Thus, it is considerably smaller than the energy of chemical bonds.

During the absorption event, the atom would recoil due to the conservation of the sums of the momenta of the atom before the reaction and the absorbed photon. The thermal movement of an atom in a gaseous absorber leads to a Doppler broadening of the absorption line and the recoil to a shift of its maximum. Typical recoil-energies lie in the range from 10^{-5} to 10^{+2} eV¹. This interval also comprises the energy of chemical bonds, phonons, and even energetically lower areas.

For atoms bound in a system and photon momenta below the threshold of the destruction of the chemical bonds, there are different aspects coming into play. For molecular systems additional rotational and vibrational degrees of freedom can be important. Simultaneously, the Doppler broadening and the recoil of the system decrease due to the enhanced mass of the system.

Making the transition to a crystal, the Doppler broadening and the recoil of the entire system become negligible. The entire recoil-energy goes into lattice vibrations. Further, there is the possibility that the momentum of the photon is taken up by the entire crystal without producing any phonons. Such an event is called *recoil-free*. In a rigid crystal, the absorption spectrum would just show the pure absorption spectrum of the nucleus, because no phonons can be produced. For photons with very low energy, i.e., less than $1.5 \times 10^{+5}$ eV the recoil-energy is below the energy of the phonons. Classically, no vibrational modes of the crystal could be excited, thus the energy and momentum conservation could not be satisfied and the related processes could not take place. However, observations show that they do take place and that in those situations a part of the events are recoil-free. Energy and momentum conservation are guaranteed when averaging over many events². The effect and the fraction of recoil-free events have been named after its discoverer R. L. Mössbauer³.

The above discussion also plays a rôle in the scattering of x-rays or neutrons from atoms. There, the distinction between elastic and inelastic events is also known. Mössbauer used also results by Lamb about neutron scattering⁴. This is the reason for the name Mössbauer-Lamb fraction.

Of interest is not only the total intensity not contained in the Mössbauer peak but also its distribution onto the remaining spectrum. Here, Visscher⁵ derived an analytical result for the observable spectrum at zero temperature in a three dimensional crystal. He also performed numerical calculations for finite temperatures. Systems with almost two-dimensional magnetic interactions are known (interaction strength 10^4 -times stronger in the plane than between the planes). Now, it is interesting to identify systems with low-

dimensional elastic interactions. Here, one could think about ultrathin films sputtered onto the surface of a solid, a liquid, or the boundary layer between two liquids. Thus a mechanical decoupling to the substrate should be achievable at least in directions parallel to the surface.

In the following section we discuss the theoretical description of these phenomena by deriving and solving a differential equation for the spectrum. Subsequently, in section III, we evaluate the solution in harmonic approximation for the isotropic Debye model in three and two dimensions at zero and finite temperature. In two dimensions at finite temperature we find that there are no recoil-free events. The Mössbauer effect ceases to exist in the strict sense. However there is still a central peak made up of almost recoil-free events, a Quasi-Mössbauer effect. Ways how to identify two dimensional elastic behavior are discussed. In the final section we summarise our paper.

II. THEORY

Starting from the absorption spectrum of a nucleus inside a rigid crystal lattice $S_{rig}(\omega_\gamma)$, we write the observed spectrum in an elastic lattice $S(\omega_\gamma)$ as a convolution of the first with a shift spectrum: $S = I * S_{rig}$. Here, ω_γ is the circular frequency of the converted photon. The shift spectrum $I(\omega)$ comprises all the information on the modifications of the observed spectrum $S(\omega_\gamma)$ due to the dynamics of the lattice. Up to an overall factor $I(\omega)$ is the spectrum one would observe, if the nucleus' line width was exactly zero. A normalisation to one $\int d\omega I(\omega) = 1$ guarantees the conservation of the integrated intensity: $\int d\omega S(\omega) = \int d\omega S_{rig}(\omega)$.

In a crystal with N Bravais lattice sites, A atoms per elementary cell, and where the atoms are elongated in d' dimensions there are $M = NAd'$ vibrational modes with circular frequencies Ω_J with $J \in \{1, 2, \dots, M\}$. In general, the dimensionality of the crystal d is the same as that of the elongations of the atoms d' which does not exclude the possibility of doing calculations with $d \neq d'$.

The state of the crystal before (i) and after (f) the emission or absorption process can be described by a set of M numbers each $\{n\}^{i,f} = \{n_J^{i,f} : J \in \{1, 2, \dots, M\}\}$. The set of all possible changes of the state is constructed by combining every possible initial state with every possible final state (direct product). The different changes contribute to the shift spectrum $I(\omega)$ with different weights $A(\{n\}^i \rightarrow \{n\}^f)$. The shift spectrum can be expressed as the weighted mean over all changes conserving the total energy:

$$I(\omega) = \sum_{\{n\}^i} \sum_{\{n\}^f} \delta[\hbar\omega - (E^f - E^i)] A(\{n\}^i \rightarrow \{n\}^f). \quad (1)$$

In a harmonic crystal the total energy is given by:

$$E^{i,f} = \hbar \sum_J \left(n_J^{i,f} + \frac{1}{2} \right) \Omega_J. \quad (2)$$

Due to the linearity of the above expression, the energy difference in equation (1) is determined exclusively by the change

$$m_J = n_J^f - n_J^i \quad (3)$$

of the occupational numbers in the different modes but not from the state $\{n\}^i$ of the crystal before the absorption or emission process. The weight $A(\{n\}^i \rightarrow \{n\}^f)$ is equal to the absolute probability for the transition from the state $\{n\}^i$ to the state $\{n\}^f$. It is given by the product of the probability $A(\{n\}^i)$ of the crystal to be in a state $\{n\}^i$ before the process and the conditional probability $A_{\{n\}^i}(\{n\}^f)$ to reach a final state $\{n\}^f$ coming from an initial state $\{n\}^i$:

$$A(\{n\}^i \rightarrow \{n\}^f) = A(\{n\}^i)A_{\{n\}^i}(\{n\}^f). \quad (4)$$

Substitution of equations (2) and (4) into equation (1) leads to:

$$I(\omega) = \sum_{\{m\}} \delta \left(\hbar\omega - \hbar \sum_J m_J \Omega_J \right) \sum_{\{n\}^i} A(\{n\}^i) A_{\{n\}^i}(\{n\}^f), \quad (5)$$

where the elements of $\{n\}^f$ are to be replaced in accordance with equation (3). For a harmonic crystal in thermal equilibrium before the elementary process, the terms belonging to a certain mode are independent from the configuration of the rest of the system. After defining the thermally averaged – i.e., averaged with the thermal weight $P_{n_J}^J$ for having n_J^i phonons in mode J before the process⁹ – probability for the production of m_J phonons in mode J :

$$A_{m_J}^J = \sum_{i n_J} P_{i n_J}^J A_{i n_J \rightarrow i n_J + m_J}^J, \quad (6)$$

where $A_{i n_J \rightarrow i n_J + m_J}^J$ is the probability for a change of the phonon number in mode J from $i n_J$ to $i n_J + m_J$ ¹⁰, the shift spectrum can be reexpressed as:

$$I(\omega) = \sum_{\{m_J\}} \delta \left(\hbar\omega - \hbar \sum_J m_J \Omega_J \right) \prod_{J'} A_{m_{J'}}^{J'}. \quad (7)$$

The probabilities are normalised to one: $\sum_{m_J} A_{m_J}^J = 1$. Consider the shift spectrum $I^{(J)}(\omega)$ for only J active modes. The shift spectrum $I^{(0)}(\omega)$ for a nucleus in an entirely rigid crystal lattice is given by a Dirac- δ -distribution: $\delta(\omega)$. The shift spectrum $I^{(M)}(\omega)$ with all modes in action is identical to the actual shift spectrum $I(\omega)$. From equation (7) we get a recursion equation for the partial shift spectra:

$$I^{(J)}(\omega) = \sum_{m_J} A_{m_J}^J I^{(J-1)}(\omega - m_J \Omega_J). \quad (8)$$

An analogous equation is valid for the changes $\Delta I^{(J)} = I^{(J)}(\omega) - I^{(J-1)}(\omega)$ in connection with the shift amplitudes $a_{m_J}^J = A_{m_J}^J - \delta_{m_J,0}$:

$$\Delta I^{(J)}(\omega) = \sum_{m_J} a_{m_J}^J I^{(J-1)}(\omega - m_J \Omega_J). \quad (9)$$

The shift amplitudes $a_{m_J}^J$ differ from the probabilities $A_{m_J}^J$ only for $m_J = 0$. There the respective shift amplitude is smaller by one. For example $A_{m_J}^J = 0$ for all $m_J \neq 0$ and $A_0^J = 1$ signifies that no phonons are created or annihilated in mode J ; so does $a_{m_J}^J = 0$ for all m_J . Hence A_0^J is a measure for remaining in the previous state and a_0^J indicates the relative change. Because of the additional Kronecker tensor $\delta_{i,j}$ and the normalisation of the probabilities $A_{m_J}^J$, the sum over all shift amplitudes amounts to zero: $\sum_{m_J} a_{m_J}^J = 0$. Writing the shift spectrum $I^{(J)}(\omega)$ as a sum over all its changes and replacing the changes $\Delta I^{(J)}(\omega)$ of the shift spectrum by the recursion (9) yields:

$$I^{(J)}(\omega) = I^{(0)}(\omega) + \sum_{J'=1}^J \sum_{m_{J'}} a_{m_{J'}}^{J'} I^{(J'-1)}(\omega - m_{J'} \Omega_{J'}). \quad (10)$$

In case, several active branches are present, the label of the mode J is composed of a branch index j and a Bloch vector \vec{k} : $J = (j, \vec{k})$. In a transition from a discrete to a continuous description the summation over all modes J is replaced by a summation over the different modal branches and an integration over k -space. The d -dimensional integral is substituted by a one-dimensional integration over the frequencies Ω of the modes. As a correction, the density of modes $\eta_j(\Omega)$ for the corresponding branch has to be taken into account. In the following, all investigations will be carried out for a single active branch. So, with the volume V of the crystal:

$$\sum_J \rightarrow V \int \frac{d^d k}{(2\pi)^d} \rightarrow \int d\Omega \eta(\Omega). \quad (11)$$

With the dispersion relation $\Omega(\vec{k})$ the density could be given by⁶:

$$\eta(\Omega) = V \int \delta[\Omega - \Omega(\vec{k})] \frac{d^d k}{(2\pi)^d}. \quad (12)$$

It can be interpreted as the total number of modes in the infinitesimally small interval $[\Omega, \Omega + d\Omega]$. The modes are counted in the entire crystal and not only in a unit volume. So, the density of modes grows proportionally to the number N of Bravais lattice sites. It is to vanish for frequencies outside the intervall $[0, \Omega_M]$. When connected to the discrete description this must also be the interval in which lie all the modal frequencies Ω_J with $J \in \{1, 2, \dots, M\}$. In the Debye model, Ω_M is equal to the Debye frequency Ω_D . For simple models, the alternative to marking the shift spectrum $I^{(J)}(\omega)$ and the shift amplitudes $a_{m_J}^J$ with the mode index J is to express them as functions of the modal frequency Ω_J : $I^{(J)}(\omega) = I(\Omega_J, \omega)$ and $a_{m_J}^J = a_m(\Omega_J)$. During the transition from the discrete to the continuous description the discrete parameter Ω_J is replaced by the continuous Ω . Values at $\Omega = \Omega_J$ for all $J \in \{1, 2, \dots, M\}$ are preserved: $\Omega_J, J \in \{1, 2, \dots, M\} \rightarrow \Omega \in [0, \Omega]$, $I(\Omega_J, \omega) \rightarrow I(\Omega, \omega)$, and $a_m(\Omega_J) \rightarrow a_m(\Omega)$. Carrying out the continuum limit in equation (10) leads to:

$$I(\Omega, \omega) = \delta(\omega) + \int_0^\Omega d\Omega' \eta(\Omega') \sum_m a_m(\Omega') I(\Omega', \omega - m\Omega'). \quad (13)$$

Here – for the sake of simplicity – we anticipate a result that will be derived later on: The shift amplitudes $a_m(\Omega)$ for fixed argument are proportional to integer negative powers of the number N of Bravais lattice sites: $a_m(\Omega) \sim N^{-|m|}$ for all $m \neq 0$ and $a_0(\Omega) \sim N^{-1}$. The shift amplitudes occur only combined in a product with the density of modes. As already stated above, the density of modes is proportional to the number N of Bravais-lattice sites. So, only the three terms with $|m| \leq 1$ survive taking the continuum limit. Two of the three shift amplitudes that are left can be expressed as functions of the third: They can be eliminated with the help of the normalisation of the shift amplitudes and because we are assuming thermal equilibrium: $a_{-m}(\Omega) = e^{-m\beta\hbar\Omega} a_{+m}(\Omega)$, respectively, where $\beta = k_B T$. Partial differentiation of equation (13) with respect to the maximum frequency Ω together with the above facts leads to a linear, first-order, non-local, partial differential equation:

$$\frac{\partial}{\partial \Omega} I(\Omega, \omega) = \eta(\Omega) a_{+1}(\Omega) \{ e^{-\beta\hbar\Omega} I(\Omega, \omega + \Omega) - (e^{-\beta\hbar\Omega} + 1) I(\Omega, \omega) + I(\Omega, \omega - \Omega) \}, \quad (14)$$

with the starting condition $I(0, \omega) = \delta(\omega)$. A Fourier transformation from the variable ω to the variable ϕ and a subsequent division through the Fourier transformed shift spectrum $\tilde{I}(\Omega, \phi)$ leads to an ordinary first-order differential equation:

$$\frac{d}{d\Omega} \ln \{ \tilde{I}(\Omega, \phi) \} = \eta(\Omega) a_{+1}(\Omega) \{ e^{-\beta\hbar\Omega} (e^{+i\phi\Omega} - 1) + (e^{-i\phi\Omega} - 1) \}. \quad (15)$$

The actual shift spectrum $I(\omega)$ is equal to $I(\Omega = \Omega_M, \omega)$. Taking into account the Fourier transformed boundary condition $\tilde{I}(\phi = 0) = 1$, we find by direct integration:

$$\tilde{I}(\phi) = \exp \left\{ \int_0^{\Omega_M} d\Omega \eta(\Omega) a_{+1}(\Omega) [e^{-\beta\hbar\Omega} (e^{+i\phi\Omega} - 1) + (e^{-i\phi\Omega} - 1)] \right\}. \quad (16)$$

Given the existence of the resulting integrals, the integral in the exponent can be separated into a ϕ -dependent and a ϕ -independent part. A Fourier retransformation yields the shift spectrum $I(\omega)$ in momentum representation:

$$I(\omega) = e^{-F} \int \frac{d\phi}{2\pi} e^{i\phi\omega} \exp \left\{ \int_0^{\Omega_M} d\Omega \eta(\Omega) a_{+1}(\Omega) [e^{(+i\phi - \beta\hbar)\Omega} + e^{-i\phi\Omega}] \right\}. \quad (17)$$

The factor e^{-F} with $F = \int_0^{\Omega_M} d\Omega \eta(\Omega) a_{+1}(\Omega) \{ e^{-\beta\hbar\Omega} + 1 \}$ is equal to the Mössbauer-Lamb fraction. The exponential series is uniformly convergent on every bounded area of the complex plane. So, as long as the magnitude of the exponent is finite, the exponential series can be integrated term by term:

$$I(\omega) = e^{-F} \sum_{\nu=0}^{\infty} \frac{1}{\nu!} \int \frac{d\phi}{2\pi} e^{i\phi\omega} \left\{ \int_0^{\Omega_M} d\Omega \eta(\Omega) a_{+1}(\Omega) [e^{(+i\phi - \beta\hbar)\Omega} + e^{-i\phi\Omega}] \right\}^{\nu}. \quad (18)$$

Reinterpretation of the inner integration as an additional Fourier transformation and decomposition of the sum into single terms $I_{\nu}(\omega)$ results in:

$$I_\nu(\omega) = \frac{e^{-F}}{\nu!} \frac{\mathcal{F}_{\phi \rightarrow -\omega}}{2\pi} \left\{ \mathcal{F}_{\Omega \rightarrow -\phi} [\eta(\Omega) a_{+1}(\Omega) e^{-\beta \hbar \Omega}] + \mathcal{F}_{\Omega \rightarrow +\phi} [\eta(\Omega) a_{+1}(\Omega)] \right\}^\nu, \quad (19)$$

where $\mathcal{F}_{\omega \rightarrow +\phi}$ denotes a Fourier transformation and where $(2\pi)^{-1} \mathcal{F}_{\phi \rightarrow -\omega}$ is its inverse. The evaluation of the first two terms is independent of the form of the density of modes or the shift amplitude:

$$\begin{aligned} I_0(\omega) &= e^{-F} \delta(\omega) \\ I_1(\omega) &= e^{-F} \left\{ \eta(-\omega) a_{+1}(-\omega) e^{+\beta \hbar \omega} + \eta(+\omega) a_{+1}(+\omega) \right\}. \end{aligned} \quad (20)$$

Terms with $\nu \geq 2$ could be reexpressed with the help of the binomial theorem and by noting that products become convolutions after a Fourier transformation. Then one sees that the term with index ν contains the effect of events on the shift spectrum during which ν phonons are converted, i.e., created or annihilated.

III. APPLICATION

Now, we would like to evaluate explicitly the shift spectrum $I(\omega)$ in harmonic approximation for the isotropic Debye model. The Debye model is based on the assumption that the crystal is a d -dimensional hypercubic lattice. So, it is a Bravais-crystal in which no optical modes exist. Isotropy leads to degenerate modes on all $d' = d$ branches. The frequencies follow a linear dispersion relation: $\Omega(\vec{k}) = sk$ with the speed of sound s and the absolute value k of the wave-number vector \vec{k} . Additionally, the integration over the first Brillouin zone is replaced by an integration over the volume of a sphere in k -space. The size of the sphere is chosen in such a way that it contains N allowed wave-number vectors where N is the number of ions in the crystal. Evaluation of equation (12) under these assumptions leads to:

$$\eta(\Omega) = d^2 \frac{N}{\Omega_D} \left(\frac{\Omega}{\Omega_D} \right)^{d-1} \theta(\Omega_D - \Omega) \theta(\Omega), \quad (21)$$

with the Debye frequency $\Omega_D = sk_D$. As mentioned above, the Debye frequency replaces the maximal frequency Ω_M . The transition probabilities which are the thermally averaged absolute squares of the transition matrix-elements $\langle \{n'_J + m'_J\} | e^{iqx} | \{n'_J\} \rangle$ are to be evaluated in a harmonic system. Here, q stands for the momentum transfer and x for the spatial coordinate along its direction. After some calculations one finds:

$$A_{m_J}^J = e^{+m_J \beta \hbar \Omega_J / 2} \exp \left\{ -\rho^J \coth \left(\frac{\beta \hbar \Omega_J}{2} \right) \right\} I_{m_J} \left\{ \rho^J \left[\sinh \left(\frac{\beta \hbar \Omega_J}{2} \right) \right]^{-1} \right\} = a_{m_J}^J + \delta_{J,0}, \quad (22)$$

with the parameter:

$$\rho^J = \frac{1}{N} \frac{(\hbar q)^2}{2M_{ion}\hbar\Omega_J}, \quad (23)$$

and where I_m stands for the modified Bessel function of the first kind and M_{ion} for the mass of the ion whose nucleus absorbs the γ -photon. For small arguments, we could use the lowest order approximation to the Bessel functions: $I_m(w) = (w/2)^m/m! + \mathcal{O}(w^{m+2})$. However, the argument of the Bessel function is divergent for a vanishing circular frequency Ω . Due to the periodic boundary conditions there exists a minimal circular frequency Ω_1 which, for a constant volume density of atoms n , depends on the total number of atoms according to: $\Omega_1 = \Xi N^{-1/d}$. The constant of proportionality Ξ depends on the geometry of the lattice and for a d -dimensional hypercubic lattice is given by $\Xi = 2\pi sn^{-1/d}$. For large N , the argument of the Bessel function becomes: $w = 2q^2 N^{(2-d)/d} / (M_{ion}\beta\Xi^2)$. In three dimensions it goes to zero as N goes to infinity. In two dimensions it is independent of the number of atoms N , so for the validity of the lowest order approximation we have to postulate additionally: $2q^2 / (M_{ion}\beta\Xi^2) \ll 1$. In one dimension the argument w is not boundend from above and so the lowest order approximation is not adequate. In every case where the lowest order approximation is justified, we have:

$$a_{m_J}^J = \frac{e^{+m_J\beta\hbar\Omega_J/2}}{|m_J|!} \left\{ \frac{\rho^J}{2} \left[\sinh\left(\frac{\beta\hbar\Omega_J}{2}\right) \right]^{-1} \right\}^{|m_J|} \sim N^{-|m_J|} \quad (24)$$

for $|m_J| \geq 1$ and

$$a_0^J = -\rho^J \coth\left(\frac{\beta\hbar\Omega_J}{2}\right) \sim N^{-1} \quad (25)$$

for $m_J = 0$. The density of modes $\eta(\Omega)$ only contributes one additional factor of N . So, if $|m_J| > 1$ the negative powers of the number of ions in the crystal cannot be compensated and the corresponding terms do not contribute. This result has already been used to derive equation (14). For vanishing absolute temperature, the above expansion is always legitimate and one finds:

$$a_{+1}^J = +\rho^J \quad a_0^J = -\rho^J \quad a_{-1}^J = 0. \quad (26)$$

Finally, the transition to the continuum has to be performed as described above. Now, equation (16) can be reexpressed depending on the dimension d of the crystal:

$$\tilde{I}_d(\phi) = \exp \left\{ \frac{\sigma_d}{\Omega_D^{d-1}} \int_0^{\Omega_D} d\Omega \Omega^{d-2} \left[\coth\left\{\frac{\beta\hbar\Omega}{2}\right\} (\cos\{\phi\Omega\} - 1) - i \sin\{\phi\Omega\} \right] \right\} \quad (27)$$

with the parameter: $\sigma_d = (dq\hbar)^2 / (2M_{ion}\hbar\Omega_D)$. The aforementioned separation into a ϕ -dependent and a ϕ -independent part without leaving a non-integrable pole in the ϕ -dependent part is possible in three dimensions at any temperature and in two dimensions

for zero temperature. The analytic expression for the exponent F_d of the Mössbauer-Lamb fraction is given by:

$$F_d = \frac{\sigma_d}{\Omega_D^{d-1}} \int_0^{\Omega_D} d\Omega \Omega^{d-2} \coth \left\{ \frac{\beta \hbar \Omega}{2} \right\} \quad (28)$$

which for zero temperature is equal to $F_d^0(\Omega_D) = \sigma_d/(d-1)$ and for non-zero temperature and in three dimensions reads:

$$F_3 = \sigma_3 \left[\frac{\ln(1 - e^{+\beta \hbar \Omega_D})}{\beta \hbar \Omega_D} - \frac{\text{dilog}(e^{+\beta \hbar \Omega_D}) + \text{dilog}(1 - e^{+\beta \hbar \Omega_D})}{(\beta \hbar \Omega_D)^2} + \frac{\pi^2}{6(\beta \hbar \Omega_D)^2} \right] \quad (29)$$

where the dilogarithm is defined as in chapter 27.7 of reference⁷. For the subset of cases investigated up to the present, the exponent is bounded and the Fourier retransformation can be carried out term by term for the exponential series. The integrated contributions $\tilde{I}_{d,\nu}(\phi = 0)$ follow a Poissonian distribution with a mean value equal to F_d . So, this parameter determines how fast the series converges. For zero temperature the retransformations for all the terms of the series can be carried out exactly:

$$I_{3,\nu}^0(\omega) = \frac{e^{-\sigma_3/2}}{\Omega_D} \sum_{\mu_1=0}^{\nu} \sum_{\mu_2=0}^{\mu_1} \frac{(-1)^{\mu_1} \sigma_3^{\nu}}{\nu!(2\nu - \mu_2 - 1)!} \binom{\nu}{\mu_1} \binom{\mu_1}{\mu_2} \theta \left(\frac{\omega}{\Omega_D} - \mu_1 \right) \left(\frac{\omega}{\Omega_D} - \mu_1 \right)^{2\nu - \mu_2 - 1} \quad (30)$$

(see figure 1) and

$$I_{2,\nu}^0(\omega) = \frac{e^{-\sigma_2}}{\Omega_D} \sum_{\mu=0}^{\nu} \frac{(-1)^{\mu} \sigma_2^{\nu}}{\nu!(\nu - 1)!} \binom{\nu}{\mu} \theta \left(\frac{\omega}{\Omega_D} - \mu \right) \left(\frac{\omega}{\Omega_D} - \mu \right)^{\nu-1} \quad (31)$$

(see figure 2). The integrations in the three dimensional case and at finite temperatures can be carried out after approximating the hyperbolic cotangent by:

$$\coth \left\{ \frac{\beta \hbar \Omega}{2} \right\} \approx 1 + 2 \frac{e^{-\beta \hbar \Omega/2}}{\beta \hbar \Omega}. \quad (32)$$

An expansion into partial fractions leads to (see figure 3):

$$\begin{aligned} I_{3,\nu}(\omega) \approx & \sum_{\mu_1=0}^{\nu} \sum_{\mu_2=0}^{\mu_1} \sum_{\lambda_1=1}^{\nu} \Lambda'_{1,\lambda_1} (-\omega')^{\lambda_1-1} e^{+\beta \hbar \Omega_D \omega'} \theta(-\omega') + \\ & + \sum_{\lambda_2=1}^{2(\nu-\mu_2)} \Lambda'_{2,\lambda_2} (+\omega')^{\lambda_2-1} \theta(+\omega') + \\ & + \sum_{\lambda_3=1}^{\nu-\mu_2} \Lambda'_{3,\lambda_3} (+\omega')^{\lambda_3-1} e^{-\beta \hbar \Omega_D \omega'} \theta(+\omega') \end{aligned} \quad (33)$$

with the factors independent of $\omega' = 2\mu_2 - \mu_1 + \omega/\Omega_D$ defined as:

$$\Lambda'_{(1,2,3),\lambda} = e^{-F} \frac{1}{\Omega_D} \frac{\sigma_3^\nu}{\nu!} \left(\frac{\beta\hbar\Omega_D}{2} \right)^{2\nu-\mu_1} \binom{\nu}{\mu_1} \binom{\mu_1}{\mu_2} e^{-\mu_2\beta\hbar\Omega/2} \frac{\Lambda_{(1,2,3),\lambda}}{\Omega_D^{4\nu-\mu_1-\lambda}} \frac{(-1)^\lambda}{(\lambda-1)!} \quad (34)$$

and where the coefficients $\Lambda_{(1,2,3),\lambda}$ are given by:

$$\begin{aligned} \Lambda_{1,\lambda_1} &= \frac{1}{(\lambda_1-1)!} \left. \frac{d^{\nu-\lambda_1}}{d\phi^{\nu-\lambda_1}} \right|_{i\phi=+\beta\hbar} \frac{p^{\mu_1-\mu_2}(\phi)}{(-i\phi)^{2(\nu-\mu_2)}(-i\phi-\beta\hbar)^{\nu-\mu_2}} \\ \Lambda_{2,\lambda_2} &= \frac{1}{(\lambda_2-1)!} \left. \frac{d^{2(\nu-\mu_2)-\lambda_2}}{d\phi^{2(\nu-\mu_2)-\lambda_2}} \right|_{\phi=0} \frac{p^{\mu_1-\mu_2}(\phi)}{(-i\phi-\beta\hbar)^{\nu-\mu_2}(+i\phi-\beta\hbar)^\nu} \\ \Lambda_{3,\lambda_3} &= \frac{1}{(\lambda_3-1)!} \left. \frac{d^{\nu-\mu_2-\lambda_3}}{d\phi^{\nu-\mu_2-\lambda_3}} \right|_{i\phi=-\beta\hbar} \frac{p^{\mu_1-\mu_2}(\phi)}{(-i\phi)^{2(\nu-\mu_2)}(+i\phi-\beta\hbar)^\nu} \end{aligned} \quad (35)$$

with the polynomial in ϕ :

$$p(\phi) = -i\phi^3(\beta\hbar\Omega_D + e^{-\beta\hbar\Omega_D/2}) - \phi^2\beta\hbar(1 - e^{-\beta\hbar\Omega_D/2}/2) - i\phi(\beta\hbar)^2(\beta\hbar\Omega_D/4) - (\beta\hbar)^3/4 \quad (36)$$

For the two-dimensional case at finite temperatures, the separation into a ϕ -dependent and a ϕ -independent part is no longer possible without leaving behind a non-integrable pole. Actually, the Mössbauer-Lamb fraction e^{-F} is exactly equal to zero because its exponent diverges. Hence, there is no recoil-free emission in this case. For further evaluation, we start by separating off the shift spectrum for zero temperature from that for finite temperature:

$$\tilde{I}_2(\phi) = \tilde{I}_2^0(\phi) \exp \left\{ 2 \frac{\sigma_2}{\Omega_D} \int_0^{\Omega_D} d\Omega \frac{e^{-\beta\hbar\Omega}}{1 - e^{-\beta\hbar\Omega}} (\cos\{\phi\Omega\} - 1) \right\} \quad (37)$$

With an approximation analogous to that in equation (32) one finds:

$$\tilde{I}_2(\phi) \approx \tilde{I}_2^0(\phi) \frac{(\beta\hbar\Omega_D/2)^2}{(\beta\hbar\Omega_D/2)^2 + (\phi\Omega_D)^2} \exp \left\{ 2 \frac{\sigma_2}{\beta\hbar\Omega_D} [E_1(\beta\hbar\Omega_D/2) - \text{Re}\{E_1[(\beta\hbar/2 \pm i\phi)\Omega_D]\}] \right\}, \quad (38)$$

where the exponential integral function E_1 is defined as in chapter 5 of reference⁷:

$$E_1(z) = \int_z^\infty dt \frac{e^{-t}}{t}. \quad (39)$$

The following integrations cannot be performed analytically, due to the exponential integral function E_1 . For the two dimensional case we had already postulated that σ_2 is to be small compared to one. In the physically interesting case of absolute temperatures T small compared to the Debye temperature $\Theta_D = \hbar\Omega_D/k_B$, the exponent as such becomes

extremely small and the exponential function can be approximated by one. In the low-temperature approximation it remains to perform the Fourier retransformation of the power of the Lorentz distribution. However, the asymptotic form of this function for large ϕ is given by $[\beta\hbar/(2\phi)]^{-2\sigma_2/(\beta\hbar\Omega_D)}$. Due to the small absolute values of the exponent this function decays slower than ϕ^{-1} which renders the Fourier retransformation difficult. Let us introduce an additional factor which ensures the convergence of the integral under investigation. If this manoeuvre is performed in a suitable way, the observable spectrum $S(\omega_\gamma)$ can be obtained directly. When choosing a Lorentz distribution as a model for the natural line shape of the nucleus, the observable spectrum is just the convolution of the former with the shift spectrum $I(\omega)$ in momentum representation. This corresponds to a multiplication of the Fourier transformed shift spectrum $\tilde{I}(\phi)$ with the Fourier transformed Lorentz distribution, i.e., a Laplace distribution also known as a doubly-exponential distribution. What remains to be executed is:

$$S_2(\omega) \approx S_0 I_2^0(\omega) * \int \frac{d\phi}{2\pi} e^{i\phi(\omega-\omega_0)} e^{-\zeta|\phi|} \left(\frac{(\beta\hbar\Omega_D/2)^2}{(\beta\hbar\Omega_D/2)^2 + (\phi\Omega_D)^2} \right)^{\frac{\sigma_2}{\beta\hbar\Omega_D}}, \quad (40)$$

with the resonance frequency of the nucleus ω_0 , the natural line-width ζ (half-width half-maximum) and the integrated intensity S_0 . The integral can be interpreted as a Laplace transformation and yields (see⁸ and figure 5):

$$S_2(\omega) \approx \frac{\beta\hbar S_0}{2\pi} I_2^0(\omega) * \text{Re} \left\{ L_{\frac{1}{2} - \frac{\sigma_2}{\beta\hbar\Omega_D}} \left(\frac{\beta\hbar[\zeta - i(\omega - \omega_0)]}{2} \right) \right\}, \quad (41)$$

with:

$$L_l(z) = 2^{l-1} \sqrt{\pi} \Gamma \left(l + \frac{1}{2} \right) z^{-l} [\text{H}_l(z) - \text{Y}_l(z)], \quad (42)$$

where $\text{H}_l(z)$ denotes the Struve function (see chapter 12 of reference⁷), $\text{Y}_l(z)$ stands for a Bessel function of the second kind also known as Weber function (see chapter 9 of reference⁷), and $\Gamma(z)$ represents the Γ -function. In the limit of vanishing line width ζ , the real part of the argument of $L_l(z)$ is equal to zero. Now, the approximation to what shall be called the *Quasi-Mössbauer line* of the shift spectrum is the convolution of the zeroth order term of the shift spectrum for zero temperature $I_{2,\nu=0}^0(\omega)$ with the line shape given by equation (41) with S_0 , ω_0 , and ζ set to zero (see figure 4):

$$I_{2,\nu=0}^T(\omega) \approx \frac{e^{-\sigma_2} \beta\hbar\Omega_D}{\Omega_D 2\pi} \text{Re} \left\{ L_{\frac{1}{2} - \frac{\sigma_2}{\beta\hbar\Omega_D}} \left(\frac{\beta\hbar[\zeta - i(\omega - \omega_0)]}{2} \right) \right\}. \quad (43)$$

IV. RESULTS

In three dimensions there is largely agreement between the present work and⁵. Here, a deeper insight has been permitted due to the presentation of the results in an analytic form. The investigations have been extended to incorporate the two dimensional case at zero and

at finite temperature respectively. The one-dimensional case at zero temperature is also covered but not investigated any further here.

In the two dimensional case at finite absolute temperatures, the Mössbauer-Lamb fraction according to its definition (17) vanishes exactly. No recoil-free absorption or emission takes place and strictly speaking, there is no Mössbauer line in the spectra. The mathematical investigation carried out here in this case is only applicable for small values of the model parameter σ_2 . But even then the execution of the calculations was not possible in the same way as for the other cases (three dimensions and/or zero absolute temperature). An alternative way had to be pursued. Although a Mössbauer line does not exist, a central peak is found. Already in the shift-spectrum representation this Quasi-Mössbauer peak shows a finite width. The width depends on the model parameter σ_2 and the temperature T .

The disappearance of the Mössbauer-Lamb fraction in two dimensions and at finite absolute temperature signifies that no entirely recoil-free events are possible and that there cannot be a Mössbauer peak. Its replacement, the Quasi-Mössbauer line must be based on quasi-recoil-free processes. These are events during which only very little energy is transformed into lattice vibrations. This could be due to the predominant creation and annihilation of low-energy phonons. Another more general possibility is based on a dominance of multi-phonon events with small net energy. In the two-dimensional case, as opposed to the three-dimensional, the density of modes does not drop rapidly enough for small absolute values of the circular frequency in order to compensate the pole of the shift amplitudes. This indicates that the first of the two explanations given above is the decisive one but does not rule out the second. The different mechanism of formation in two dimensions leads to a central peak of finite width depending on the temperature. In the representation as observable spectrum, i.e., after the convolution of the shift spectrum with the natural line shape, the Mössbauer and the Quasi-Mössbauer line appear qualitatively similar (see figure 4). Quantitatively they are not. They differ in peak height, line width, and integrated intensity. Given the qualitative similarity, the calculations would have to be reperformed with a more realistic than the Debye model in order to obtain more reliable quantitative results.

While the phonon wings might render the determination of the central line's integrated intensity cumbersome, they provide the best means to identify two-dimensional elastic behavior (see figure 5). For narrow spectra, in three dimensions, the phonon wing passes through a relative minimum almost reaching down to zero close to the central peak. In two dimensions a nearly horizontal passage can be seen. This means also that the phonon wings for positive and negative circular frequencies are continuously connected at zero frequency in three dimensions (see also figure 3). In two dimensions there is a step (see figure 5).

Room for extension of the present work lies in the investigation of slowly decaying spectra in two dimensions.

Acknowledgements

Help by R. J. Jelitto is gratefully acknowledged.

- ¹ G. K. Wertheim, *Mössbauer Effect: Principles and Applications*, Academic Press, New York (1964).
- ² H. J. Lipkin, *Annals of Physics* **9**, 332-339 (1960).
- ³ R. L. Mössbauer, *Z. Naturforschg.* **14** 211-216 (1959).
- ⁴ W. E. Lamb, *Phys. Rev.* **55** 190 (1939).
- ⁵ W. M. Visscher, *Annals of Physics* **9**, 194-210 (1960).
- ⁶ N. W. Ashcroft and N. D. Mermin, *Solid State Physics*, Chap.23, Saunders College Publishing, (1976).
- ⁷ M. Abramowitz and I. A. Stegun, *Handbook of Mathematical Functions*, Dover, New York (1972).
- ⁸ A. Erdelyi, W. Magnus, F. Oberhettinger, and F. G. Tricomi, *Tables of Integral Transforms*, Chapter 4.3(10), McGraw-Hill, New York (1953).
- ⁹ In thermal equilibrium: $A(\{n\}_i) = \prod_J P_{n_j^i}^J$.
- ¹⁰ The probability for the change of two configurations of the crystal into another is given by the product of the probabilities for the respective changes in all the modes: $A_{\{n\}_i}(\{n\}_f) = \prod_J A_{n_j^i \rightarrow n_j^f}^J$.

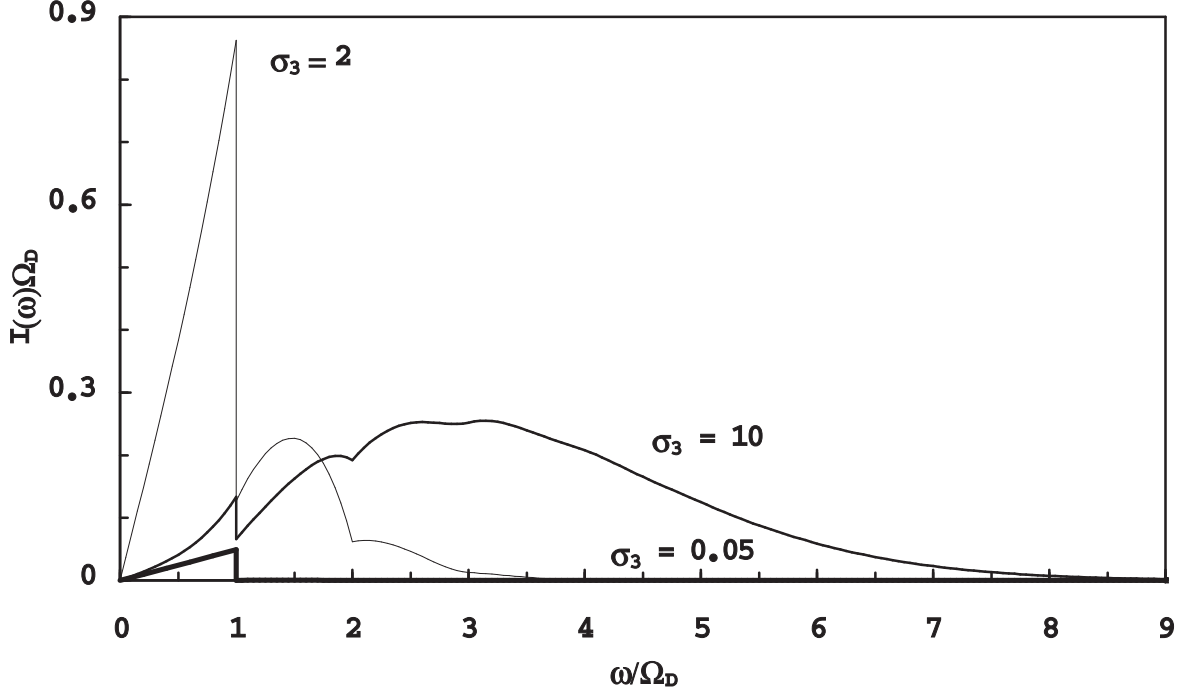


FIG. 1: The figure shows the shift spectrum $I(\omega)$ in three dimensions and for zero temperature. Different values of the model parameter σ_3 have been chosen. The abscissa and the ordinate are rescaled with the Debye frequency Ω_D . In an unscaled presentation, a variation of the Debye frequency Ω_D with the parameter σ_3 kept constant would lead to variations of the aspect ratio of the graph. The step structure inherent to the shift spectrum with steps at integer multiples of the Debye frequency emerges from the plot. For smaller values of the Mössbauer-Lamb fraction these steps are smoothed out more and more until the spectrum resembles a Poissonian or Gaussian distribution. For large Mössbauer-Lamb fractions apart from the Mössbauer line which coincides with the axis in this plot, the spectrum mainly only consists of a small contribution between zero and the Debye frequency Ω_D . At zero temperature, the shift spectrum is identical to zero for negative values of the frequency ω , because there is no initial population of the crystal with phonons which could be annihilated. Especially the sharp peak at $\omega = \Omega_D$ can be traced back to the use of the Debye model and would be less pronounced for a model with an adapted behavior for higher phonon frequencies.

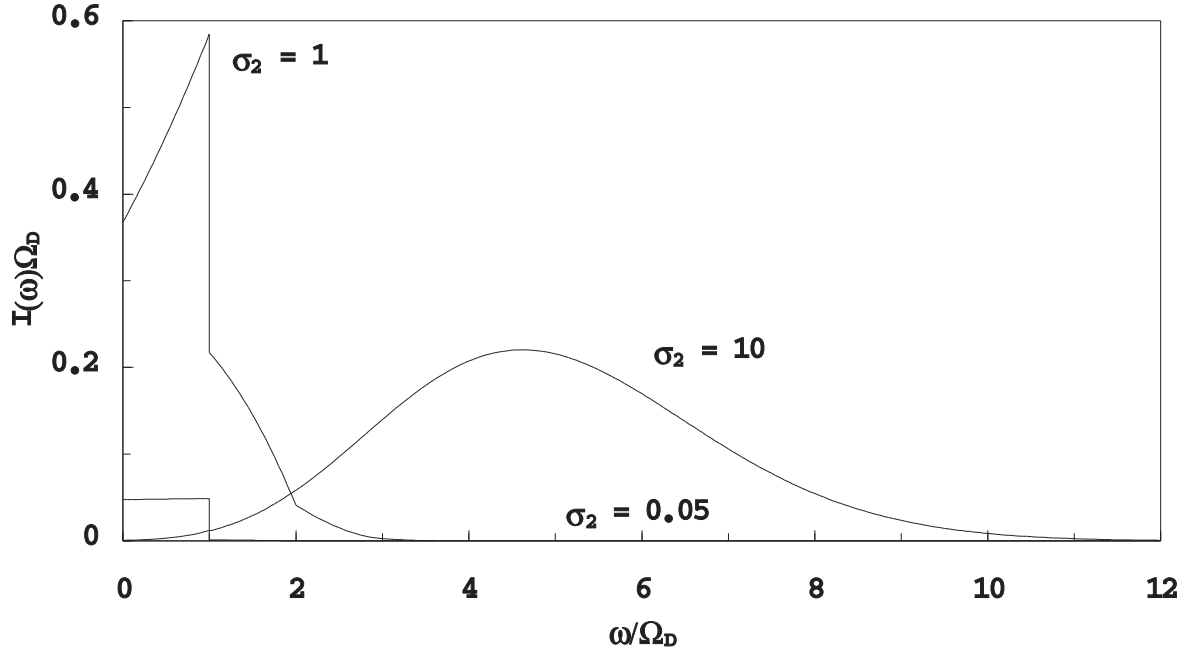


FIG. 2: Here, the shift spectrum $I(\omega)$ for two dimensions is depicted for zero temperature, where various values have been chosen for the model parameter σ_2 . The scaling properties and the step structure are equally well discernible as in figure 1. The transition to a Poissonian or Gaussian like distribution for slowly decaying spectra becomes evident, too. The difference to the three-dimensional case lies in the details of the different contributions. The spectrum for the highest Mössbauer-Lamb fraction in two dimensions shows an almost constant passage from zero frequency to the Debye frequency Ω_D whereas in three dimensions it shows a linearly rising behaviour.

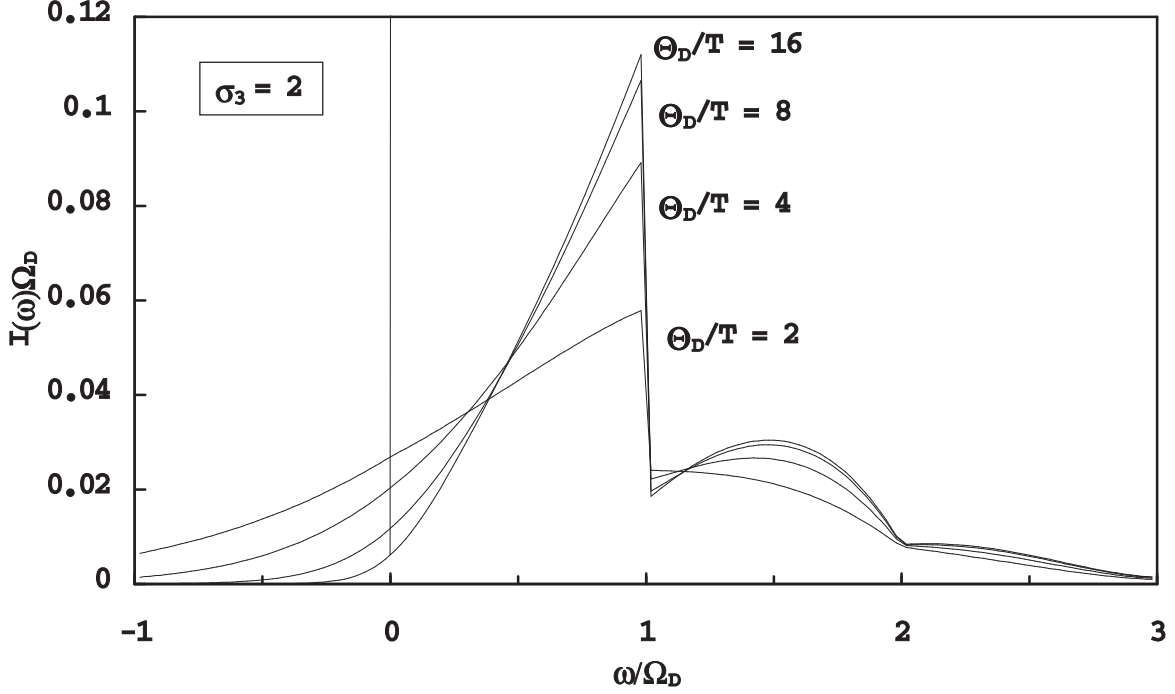


FIG. 3: In this figure, the shift spectrum $I(\omega)$ is presented for different values of the absolute temperature T and the model parameter: $\sigma_3 = 2$. For zero absolute temperature the corresponding plot is given in figure 1. The shift spectrum only depends on the ratio of the absolute temperature to the Debye temperature Θ_D . For the shown cases with relatively low temperatures, the step structure known from figure 1 is conserved. However, for increasing temperature it becomes smoother. The scaling behaviour with the Debye frequency Ω_D also remains the same, only that additionally, the ratio between the absolute and the Debye temperature Θ_D has to be kept constant. Now there are also contributions for negative circular frequencies ω . They belong to those events where net energy is drawn from the crystal.

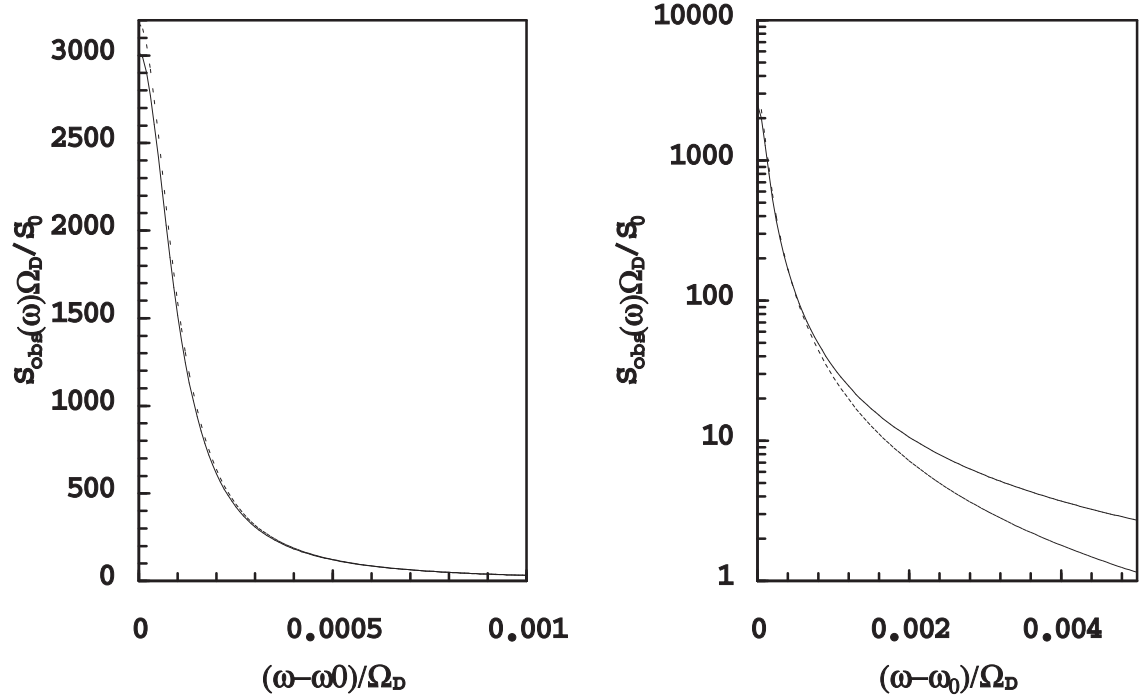


FIG. 4: The two figures 4 serve as a comparison between the Quasi-Mössbauer line in two dimensions and the Mössbauer line in three dimensions for the same choice of the physical constants: $\sigma_3 = 0.05 = (9/4)\sigma_2$, $\beta\hbar\Omega_D = 10$, and $\zeta/\Omega_D = 10^{-4}$. The two graphs show the observable spectrum $S_{obs}(\omega)$ rescaled with the Debye frequency Ω_D and the integrated intensity S_0 . In order to emphasise the differences, a small natural line-width has been chosen. The lines are always even functions with respect to inversion of the sign of the argument relative to the resonance frequency ω_0 . The figure on the lhs is a doubly linear plot. Here, the slightly higher maximum value of the Mössbauer line (dashed) compared to the Quasi-Mössbauer line (solid) can be seen. For large values of the circular frequency, the Mössbauer line tends to zero faster than the Quasi-Mössbauer line. This can best be seen in the figure on the rhs which has a logarithmic ordinate. The two lines do not have the same integrated area. The area beneath the Mössbauer line is larger by a factor of $e^{(7/4)\sigma_3}$. On first sight, the two lines do not differ in their width. Numerically a difference of a Quasi-Mössbauer line with a 0.4 percent larger width is found. This value can be increased to 3 percent for the smallest natural line width found in nature ($\zeta/\Omega_D = 10^{-11}$). In the last case however, the absolute difference is one million times smaller.

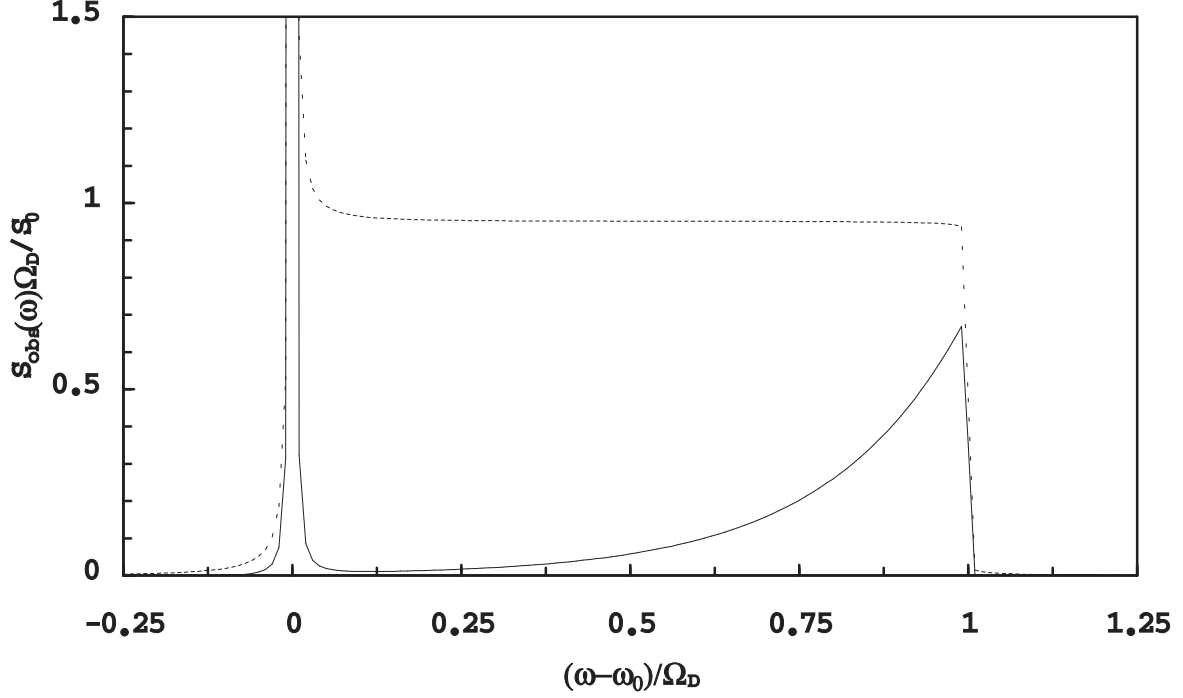


FIG. 5: In this figure, the graphs of the following two observable spectra $S_{obs}(\omega)$ at finite temperature are depicted: The one for two dimensions (dashed) with the model parameter set to $\sigma_2 = 1/45$ and the other for three dimensions (solid) with the model parameter $\sigma_3 = 1/20$. The other parameters defining the temperature and the natural line-width respectively are: $\beta\hbar\Omega_D = 10$ and $\zeta/\Omega_D = 10^{-4}$. The spectrum in two dimensions decays more slowly for negative values of the circular frequency ω than in three dimensions. The most pronounced difference can be found for the circular frequency between zero and the Debye frequency Ω_D . There, the contribution of the first order of the expansion of the exponential function shows up. In three dimensions, the observable spectrum $S_{obs}(\omega)$ passes through a relative minimum almost reaching down to zero. In two dimensions, a nearly horizontal passage can be seen. This interval is the most suitable place to distinguish between the two cases by measurements and to identify two-dimensional elastic behaviour.